Organic Process Research & Development **2005**, *9*, 768–773

The Model of Catalytic Reactor of Ethylene Glycol Production

V. F. Shvets, R. A. Kozlovskiy,* I. A. Kozlovskiy, M. G. Makarov, J. P. Suchkov, and A. V. Koustov

D. I. Mendeleev University of Chemical Technology of Russia, Chair of Basic Organic and Petrochemical Synthesis, 9 Miusskaya Square, Moscow 125047, Russia

Abstract:

The ethylene oxide hydration process in a catalytic fixed bed tube reactor was studied. A cross-linked styrene-divinylbenzene anion-exchange resin in the HCO_3^-/CO_3^{2-} -form was used as a catalyst. The deactivation and swelling of the catalyst during the process were detected. The mathematical model of the reactor with determined parameters adequately describing the rate of the reaction, product distribution and catalyst deactivation and swelling has been developed.

Introduction

Hydration of ethylene oxide is an industrial approach to glycols in general, and ethylene glycol in particular. Ethylene glycol is one of the major large-scale products of industrial organic synthesis, with the world annual production of about 15.3 million ton/y in 2000.[1] Hydration of ethylene oxide proceeds on a serial-to-parallel route with the formation of homologues of glycol:

$$H_2O \xrightarrow[k_0]{C_2H_4O} HOCH_2CH_2OH \xrightarrow[k_1]{C_2H_4O} HO(CH_2CH_2O)_2H \xrightarrow[k_2]{C_2H_4O} \text{etc.} \quad \text{(I)}$$

where k_0, k_1, k_2 are rate constants.

Now ethylene glycol is produced in industry only by a noncatalyzed reaction. Product distribution in the reaction I is regulated by the oxide/water ratio in the initial reaction mixture. The ratio of the rate constants for the steps 2 to 1 of the reaction I is unfavorable for monoglycol formation. The distribution factor $b = k_1/k_0$ for a noncatalyzed reaction of ethylene oxide with water according to different data sources [2] is in the range of 1.9−2.8. For this reason, a large excess of water (up to 20 mol equiv) is applied to increase the monoglycol yield on the industrial scale. This results in a considerable power cost at the final product isolation stage from dilute aqueous solutions.

One of the ways of increasing the monoglycol selectivity and, therefore, of decreasing water excess is the application of catalysts accelerating only the first step of the reaction I. Typical examples of such catalysts would be the anions of salts of some acids[3−6] and metalate anions.[7−8] The kinetics and reaction mechanism of α-oxide hydration using homogeneous catalysis by the salts (acetate, formate, oxalate, carbonate, bicarbonate, etc.) have been explicitly studied.[3,10,11,32] As it is evident from the kinetic data, the distribution factor reduces 10-fold (to 0.1−0.2) at the concentration of some salts of about 0.5 mol/L. This enables production of monoglycol with high selectivity at water−oxide molar ratios close to 1.

Figure 1 presents influence of ethylene oxide-to-water ratio on the ethylene glycol yield for noncatalytic, homogeneously and heterogeneously catalyzed reactions.

Hereinafter we have explored the properties of the above-mentioned homogeneous catalysts to create the industrial heterogeneous catalysts of the selective hydration of ethylene oxide by means of an immobilization of anions of salts on heterogeneous carriers.[12−17] The largest ethylene glycol producers, such as Shell,[18−24] Dow,[25,26] BASF,[27] Union

* To whom correspondence should be addressed. E-mail: kra@muctr/edu/ru; shvets@muctr.edu.ru.

(1) Noor-Drugan, N. Testing Times for Ethylene Glycol Makers. *Chem. Week* **1999**, *March 3*, 32.
(2) Dyment, O. N.; Kazansky, K. S.; Miroshnikov, A. M. *Glycols and their derivatives* (Rus.); Moscow, **1976**.
(3) Lebedev, N. N.; Shvets, V. F.; Romashkina, L. L. *Kinet. Catal. (Rus.)* **1976**, *17*(3), 576.
(4) Masuda, T. Production of Polygydric Alcohol. JP 61-271229, 1986.
(5) Masuda, T. Production of Polygydric Alcohol. JP 61-271230, 1986.
(6) Masuda, T.; Asano, K. H.; Naomi Ando, S. Method for Preparing Ethylene Glycol and/or Propylene Glycol. EP 0226799 1992, U.S. Patent 4,937,393, 1990.
(7) Keen, B. T. Carbon Dioxide-Enhanced Monoalkylene Glycol Production. U.S. Patent 4,578,524, 1985.
(8) Keen, B. T.; Robson, J. H. Continuous Process for the Production of Alkylene Glycol in the Presence of Organometalate. U.S. Patent 4,571,-440, 1986.
(9) Odanaka, H.; Yamamoto, T.; Kumazawa, T. Preparation of High-Purity Alcylene Glycol. JP Patent 56090029, 1981.
(10) Lebedev, N. N.; Shvets, V. F.; Romashkina, L. L. *Kinet. Catal. (Rus.)* **1976**, *17*(3), 583.
(11) Lebedev, N. N.; Shvets, V. F.; Romashkina, L. L. *Kinet. Catal. (Rus.)* **1976**, *17*(4), 888.
(12) Shvets, V. F.; Makarov, M. G.; Suchkov, J. P.; et al. Method for Obtaining Alkylene Glycols. RU Patent 2001901, 1993.
(13) Shvets, V. F.; Makarov, M. G.; Suchkov, J. P.; et al. Method for Obtaining Alkylene Glycols. RU Patent 2002726, 1993.
(14) Shvets, V. F.; Makarov, M. G.; Koustov, A. V.; et al. Process for Obtaining Alkylene Glycols. WO 9733850, 1997.
(15) Shvets, V. F.; Makarov, M. G.; Koustov, A. V.; et al. Method for Obtaining Alkylene Glycols. RU Patent 2122995, 1999.
(16) Shvets, V. F.; Makarov, M. G.; Koustov, A. V.; et al. Method for Producing Alkylene Glycols. WO 9912876, 1999.
(17) Shvets, V. F.; Makarov, M. G.; Koustov, A. V.; et al. Method for Obtaining Alkylene Glycols. RU Patent 2149864, 2000.
(18) Reman, W. G.; Van Kruchten, E. M. G. Process for the Preparation of Alkylene Glycols. U.S. Patent 5,488,184, 1996.
(19) Van Kruchten, E. M. G. Process for the Preparation of Alkylene Glycols. U.S. Patent 5,874,653, 1999.
(20) Van Kruchten, E. M. G. Catalytic Hydrolysis of Alkylene Oxides. WO 9923053, 1999.
(21) Van Kruchten, E. M. G. Quaternary Phosphonium Salt Catalyst in Catalytic Hydrolysis of Alkylene Oxides. WO 0035840, 2000.
(22) Van Kruchten, E. M. G. Carboxylates in Catalytic Hydrolysis of Alkylene Oxides. WO 0035842, 2000.
(23) Kunin, R.; Lemanski, M. F.; Van Kruchten, E. M. G. Catalyst Stabilizing Additive in the Hydrolysis of Alkylene Oxides. WO 0035841, 2000.
(24) Van Kruchten, E. G. A. Catalytic Hydrolysis of Alkylene Oxides. U.S. Patent 6,137,014, 2000.
(25) Lee, G.-S.; Rievert, W. J.; Von Landon, G.; Strickler, G. R. Process for the Production of Ethelene Glycol. WO 9931033, 1999.

Published on Web 11/02/2005

10.1021/op058005+ CCC: $30.25

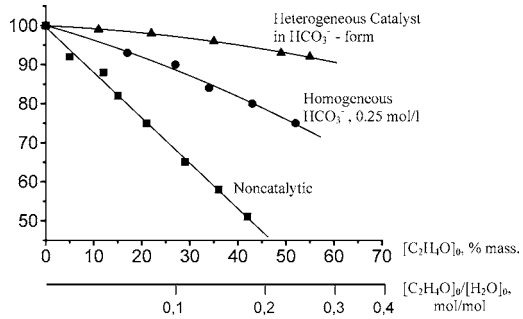

Figure 1. **Influence of the ethylene oxide-to-water ratio on the ethylene glycol yield for noncatalytic, homogeneously and heterogeneously catalyzed reactions.**

Table 1. **Properties of the anion-exchange resins**

resin	SBR	Marathon A
functional group	-[Ph-CH_2-$N(CH_3)_3$]$^+$	-[Ph-CH_2-$N(CH_3)_3$]$^+$
total exchange capacity, equiv/L	1.4	1.2
particle size, mm	0.3−1.2	0.575 ± 0,05
matrix type	gel	gel

Carbide[28−30] and Mitsubishi,[31] conduct their studies on elaboration of selective catalysts of ethylene oxide hydration in the same direction.

To optimize the conditions for the catalyst exploitation, it is necessary to have an adequate mathematical model of the heterogeneous catalytic process. The first step for creation of the model would be generation of a kinetic model of the homogeneous hydration of ethylene oxide, catalyzed by the bicarbonate anion in concentrated water solutions. Such a model was prepared in our earlier report.[32]

Experimental Section

Materials. $NaHCO_3$, ethylene glycol, diethylene glycol, and triethylene glycol were purchased from commercial suppliers and used without further purification. Ethylene oxide was purified by distillation over solid NaOH. Water was purified by distillation.

Anion-exchange resins, Dowex SBR and Dowex Marathon A, activated by anion exchanging with sodium bicarbonate solution were used as catalysts. The properties of resins are summarized in Table 1.

Apparatus. All experiments were carried out in a tubular, stainless steel laboratory reactor with a heat-exchange jacket. The volume of the reactor for each experiment is listed in Table 2, and the inner diameter of the reactor was 0.004 m in all experiments. The temperature in the reactor was maintained by circulation of the thermostatic silicone liquid through the heat-exchange jacket. Experiments were carried out at constant temperature in the range of 95−115 °C and under constant pressure in a range of 1.5−2.0 MPa.

Table 2. **Conditions of the experiments**

no	ionite	reactor volume, cm^3.	*t*, °C	$[C_2H_4O]_0$, %	$[MEG]_0$, %	run time, h
1	SBR	2.6	95	12	0	939
2	Marathon A	2.3	95	12	0	925
3	SBR	6.3	105	12	0	978
4	SBR	6.3	105	20	0	708
5	SBR	6.3	105	20	0	705
6	SBR	6.3	105	20	0	741
7	SBR	6.3	105	20	20	411
8	SBR	2.3	115	20	0	154

Analysis. Concentrations of mono-, di-, and triethyleneglycols in the reaction mixture were determined by GLC, using a 1 m × 0.003 m glass column packed with 15% FFAP on Inerton AW-DMCS (0.2−0.25 mm). 2-Ethoxyethanol was used as an internal standard.

The ethylene oxide concentration was determined by treatment of the probe with HCl in dioxane followed by titration of the excess of HCl with NaOH.[33]

The concentrations of carbonate and bicarbonate anions in the catalyst were determined by titration of the solution obtained after full ion exchange of carbonate and bicarbonate anions with chloride anion in 10% NaCl/water solution.

Results and Discussion

A series of experiments in the tubular reactor under a wide range of initial concentrations, temperatures, feed rates, and run time were carried out. The conditions of the experiments are listed in Table 2. During the experiments, composition of the outlet feed was determined, and activity and selectivity of the catalyst were calculated. As a measure of activity, the effective first-order rate constant was used:

$$k_{\text{eff}} = \frac{\ln\left(\frac{[C_2H_4O]_0}{[C_2H_4O]}\right)}{t} \qquad (1)$$

The typical form of changing activity and selectivity during the run time is presented in Figure 2.

Model of Tubular Plug-Flow Fixed-Bed Catalytic Reactor (Hydration Model). Development of the hydration model was based on the following propositions:

(i) Reaction volume consists of two phases: the liquid phase and the Ionite (catalyst) phase.

(ii) Plug-flow regime of the liquid-phase stream through the catalyst bed.

(iii) Catalytic and noncatalytic ethylene oxide hydrations take place in the Ionite phase, and only the noncatalytic reaction takes place in the liquid phase.

(iv) Distribution of the components of the reaction mixture between liquid and Ionite phases is a result of the fast equilibrium.

(26) Lee, G.-S.; Rievert, W. J.; Von Landon, G.; Strickler, G. R. Method for Making Glycol in an Adiabatic Reaction System. WO9931034, 1999.
(27) Gehrer, E.; Stein, B.; Grosch, G. Production of Alkylene Glycol by Reacting Alkylene Oxide with Water on a Catalyst. Patent DE 19757684, 1999.
(28) Soo, H.; Ream, B. C.; Robson, J. H. Monoalkylene Glycol Production Using Mixed Metal Framework Compositions. U.S. Patent 4,967,018, 1990.
(29) Soo, H.; Ream, B. C.; Robson, J. H. Mixed Metal Framework Compositions for Monoalkylene Glycol Production. U.S. Patent 5,064,804, 1990.
(30) Forkner, M. W. Monoalkylene Glycol Production Using Highly Selective Monoalkylene Glycol Catalysts. U.S. Patent 5,260,495, 1993.
(31) Iwakura, T.; Miyagi, H. Production of Alkylene Glycol. JP Patent 11012206, 1999.
(32) Kozlovsky, I. A.; Kozlovsky, R. A.; Koustov, A. V.; Makarov, M. G.; Suchkov, J. P.; Shvets, V. F. *Org. Process Res. Dev.* **2002**, *6*, 660−664.
(33) Siggia, S. ; Hanna, J. G. *Quantitative Organic Analysis via Functional Groups*, 4th ed.; Wiley: New York, 1978.

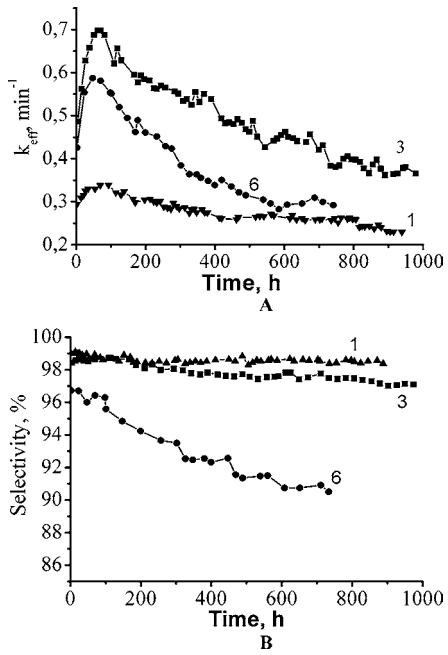

Figure 2. **(A) Changing of k_{eff} vs time. (B) Changing of selectivity vs time. Number of a curve corresponds to the number of experiments. Experimental conditions: (Curve 1) $[C_2H_4O]_0 = 12\%$ mass, 95 °C, catalyst SBR. (Curve 3) $[C_2H_4O]_0 = 12\%$ mass, 105 °C, catalyst SBR; (Curve 6) $[C_2H_4O]_0 = 20\%$ mass, 105 °C, catalyst SBR.**

(v) It was shown experimentally that there are isothermal conditions inside the reactor.

Since the reactor is considered as a plug-flow reactor, changing the molar flow (dF_j) and concentration (dC_j) of each component (j) of reaction along with the reactor volume (or holding time) can be written as follows:

$$dF_j = dV(\alpha r_{ji} + (1-\alpha) r_{jl})$$
$$dC_j = dt(\alpha r_{ji} + (1-\alpha) r_{jl}) \quad (2)$$

where $\alpha = V_i/V$ the ratio of the Ionite phase volume to the reactor volume (Ionite volume fraction); t = holding time; r = reaction rate; $_j$ = the identification mark related to the component; $_i$ = identification mark related to the Ionite phase; $_l$ = identification mark related to the liquid phase.

The kinetic equations and rate constants, the same as those for homogeneous reactions reported earlier,[32] were applied to the description of the reaction rates both in the Ionite and the liquid phases. For example, full kinetic equations for ethylene oxide consumption and ethylene glycol generation are as follows:

$$\frac{d[C_2H_4O]}{dt} = (1-\alpha)k_0([H_2O]_l + 2.6\sum[Gl]_l)([H_2O]_l + 1.84\sum[Gl]_l)[C_2H_4O]_l + \alpha(k_0[H_2O]_i + 2.6k_0\sum[Gl]_i + k_{A1}[HCO_3^-]_i + k_{A2}[CO_3^{2-}]_i + k_{HO^-}[HO^-]_i + 14k_{HO^-}[HO^-]_i \times \sum[Gl]_i/[H_2O]_i))([H_2O]_i + 1.84\sum[Gl]_i)[C_2H_4O]_i \quad (3)$$

$$\frac{d[EG]}{dt} = (1-\alpha)k_0([H_2O]_l - 2.6[EG]_l)([H_2O]_l + 1.84\sum[Gl]_l)[C_2H_4O]_l + \alpha([H_2O]_i + 1.84\sum[Gl]_i)(k_0([H_2O]_i - 2.6[EG]_i) + k_{A1}[HCO_3^-]_i + k_{A2}[CO_3^{2-}]_i + k_{HO^-}[OH^-]_i(1 - 14[EG]_i/[H_2O]_i))[C_2H_4O]_i \quad (4)$$

where: k_0 is the noncatalytic rate constant; k_{A1} is the rate constant of bicarbonate-anion catalyzed reaction; k_{A2} is the rate constant of carbonate−anion catalyzed reaction; k_{HO^-} is the rate constant of hydroxyl-anion catalyzed reaction; [EG] is the ethylene glycol concentration; Σ[Gl] is the sum of all glycol concentrations.

The same approach was applied for formulation of kinetic equations for all components of reaction mixture such as water and polyglycols.

Concentrations of the components of the liquid phase have been determined by analysis of the outlet flow. Concentrations in the Ionite phase were calculated from the following equilibrium equations:

$$\delta_1 = \frac{[SH]_i\,[C_2H_4O]_i}{[SH]_l\,[C_2H_4O]_l} \quad (5)$$

$$\delta_2 = \frac{[H_2O]_i}{[H_2O]_l} \quad (6)$$

$$\delta_3 = \frac{\sum[Gl]_i}{\sum[Gl]_l} \quad (7)$$

where $[SH] = [H_2O] + 1.84\sum[Gl]$ = total effective concentration of solvating agents.

The values of the equilibrium constants (δ_1, δ_2, and δ_3) were the only parameters determined from the experimental data using the eqs 2−4. All the other kinetic parameters were used from the kinetics acquired earlier.[32] All concentrations were determined experimentally including values of $[HCO_3^-]_i$, $[CO_3^{2-}]_i$, and $[HO^-]_i$ measured at the starting and the ending points of the long-term experiments. The data in the Table 3 show that the values of $\delta_1 \approx 1$ and $\delta_2 = \delta_3 = 0.5$ would allow to satisfactorily describe outlet component concentrations as at starting and final point of the experiment.

Thus, the system of eq 2 complemented with kinetic eqs 3 and 4 with experimentally determined parameters δ_1, δ_2, and δ_3 can serve as a mathematical model of the tube reactor for the steady state of the catalyst (marked as a Hydration Model).

Model of the Catalyst Deactivation and Swelling (Deactivation Model). In reality, the catalyst changes its state during the run time due to two undesirable processes: deactivation (loss of active sites) and swelling. Loss of the catalytic activity causes decreasing in selectivity (Figure 2.). The rates of both the deactivation and the swelling directly correlate with the changing of the temperature, as well as ethylene oxide and glycol concentrations (Figures 2 and 3, and Table 4).

To elaborate the model of the catalyst deactivation it is desirable to have the data of active-site concentration during

Table 3. **Comparison of the experimental and calculated by Hydration Model data of ethylene oxide conversion and ethylene glycol selectivity**

exp No	ionite	experiment point	δ_1	ethylene oxide conversion, % exp.	ethylene oxide conversion, % calc.	ethylene glycol selectivity, % exp.	ethylene glycol selectivity, % calc.
1	SBR	start	0.81	95.6	95.6	98.1	98.3
		finish	1.00	88.0	87.9	97.8	97.8
2	Marathon-A	start	0,96	95.3	95.3	97.6	98.4
		finish	1.28	88.5	88.5	98.0	97.2
3	SBR	start	0,89	98.1	98.1	98.2	96.9
		finish	1.09	85.9	85.9	97.1	95.5
4	SBR	start	0,76	95.8	95.8	95.6	95.3
		finish	0.97	80.1	80.1	95.2	91.2
5	SBR	start	0,81	96.4	96.4	96.2	95.3
		finish	0.92	78.2	78.2	95.0	90.4
6	SBR	start	0,82	96.7	96.7	95.9	95.5
		finish	0.94	81.4	81.4	90.5	91.4
7	SBR	start	0,89	94.8	94.8	87.3	89.6
		finish	0.95	80.6	80.6	76.4	76.1
8	SBR	start	0,64	93.6	93.6	95.3	95.3
		finish	0.53	82.5	82.5	91.5	91.2

Table 4. **Comparison of the experimental and calculated data of final active sites concentration ($C_{A,fin}$), catalyst volume ($V_{i,fin}$), and carbonate anion fraction (M_{fin})**

no	$C_{A,0}$, g-equiv/L	$C_{A,fin}$, g-equiv/L exp.	$C_{A,fin}$, g-equiv/L calc.	$V_{i,0}$, cm^3	$V_{i,fin}$, cm^3 exp.	$V_{i,fin}$, cm^3 calc.	M_0	M_{fin} exp.	M_{fin} calc.
1	1.2	0.55	0.58	1.5	2.3	2.44	0.47	0.34	0.34
2	1.09	0.42	0.53	1.6	2.5	2.5	0.47	0.4	0.35
3	1.04	0.29	0.25	1.7	3.8	2.9	0.47	0.24	0.24
4	1.03	0.17	0.12	1.7	5.65	5.0	0.47	0.27	0.29
5	0.98	0.14	0.114	1.7	6.6	5.0	0.47	0.28	0.29
6	1.02	0.18	0.11	1.7	5.6	5.1	0.47	0.28	0.29
7	0.79	0.13	0.17	1.7	6.9	7.2	0.47	0.39	0.36
8	0.96	0.29	0.27	1.0	1.6	1.7	0.47	0.39	0.42

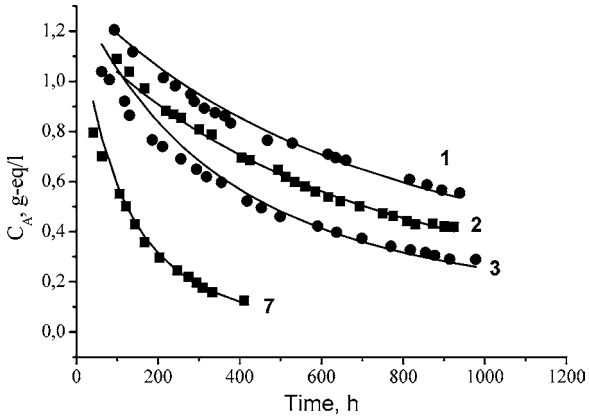

Figure 3. **Changing of active sites concentration vs run time. Dots: calculated from experimental data by Hydration Model. Lines: calculated by Deactivation Model. Number of a curve corresponds to the number of experiments.**

the run time. The aforementioned Hydration Model was used for calculation of the active-site concentrations at each experimental time point (dots in Figure 3) using the acquired data of the outlet feed composition.

Development of the Deactivation Model was based on the assumption that:

(1) active-site loss occurs due to the following cleavage reactions:

$$-[N(CH_3)_3]^+ + OH^- \rightarrow -OH + N(CH_3)_3 \quad \text{(II)}$$

$$-[N(CH_3)_3]^+ + OH^- \rightarrow -N(CH_3)_2 + CH_3OH \quad \text{(III)}$$

(2) catalyst swelling proceeds via ethylene oxide addition to active sites:

$$-N(CH_3)_2 + C_2H_4O + H_2O \rightarrow -[N(CH_3)_2C_2H_4OH]^+OH^- \quad \text{(IV)}$$

$$-[N(CH_3)_2C_2H_4OH]^+ + nC_2H_4O \xrightarrow{OH^-} -[N(CH_3)_2(C_2H_4O)_{n+1}H]^+ \quad \text{(V)}$$

$$-OH + nC_2H_4O \xrightarrow{OH^-} -O(C_2H_4O)_nH \quad \text{(VI)}$$

(3) OH^- formation occurs due to hydrolysis of anions:

$$HCO_3^- + H_2O \rightleftarrows H_2CO_3(CO_2 + H_2O) + OH^- \quad \text{(VII)}$$

$$CO_3^{2-} + H_2O \rightleftarrows HCO_3^- + OH^- \quad \text{(VIII)}$$

The following assignments were made:

(1) Active-site concentration in Ionite phase:

$$C_A = [HCO_3^-] + 2[CO_3^{2-}] \quad (8)$$

(2) Carbonate anion fraction in Ionite phase:

$$M = \frac{[CO_3^{2-}]}{[HCO_3^-] + [CO_3^{2-}]} \quad (9)$$

(3) Equilibrium concentration of OH^- -anion:

$$[OH^-] = K_h\frac{[CO_3^{2-}]}{[HCO_3^-]} = K_h\frac{M}{(1-M)} \quad (10)$$

where K_h = equilibrium constant of anion hydrolysis, which depends on temperature by the following equation:

$$K_h = \exp\left(9886 - \frac{5392}{T}\right) \text{mol/L} \quad (11)$$

The rate of the active-site cleavage can be described by the following kinetic equation with the first-order concerning hydroxyl-anion and active-site concentrations corresponding to bimolecular reaction II:

$$\frac{dC_A}{dt} = -k_d[OH^-]C_A \quad (12)$$

where k_d = rate constant of the active-site cleavage, L/(mol h).

As the catalyst mass increasing proceeds due to ethylene oxide addition, the catalyst volume changing can be expressed as follows:

$$V_i = V_{i,0} + N_{EO} \times \frac{M_{EO}}{\rho} \quad (13)$$

where: $V_{i,0}$ = initial catalyst volume; V_i = current catalyst

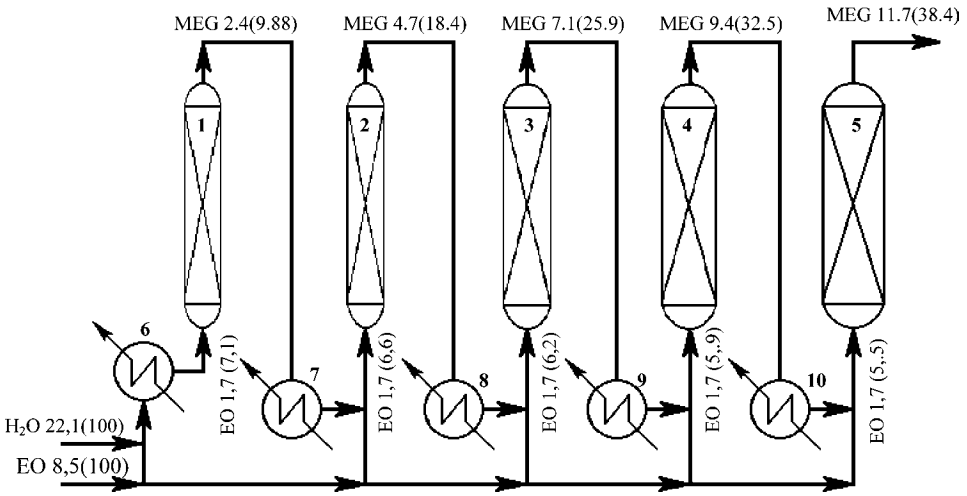

Figure 4. **Installation of ethylene glycol production. Flow scheme. EO: ethylene oxide; MEG: monoethylene glycol; Numerals on the flow: feed, ton/h; in brackets: component concentration, % mass. 1, 2, 3, 4, 5 = reactors; 6 = heater; 7, 8, 9, 10 = intermediate heat exchangers.**

volume; N_{EO} = moles of ethylene oxide added to the catalyst; M_{EO} = mole weight of ethylene oxide; ρ = density of the EO linked to the catalyst ($\rho = 0.737 \pm 0.027$ g/cm^3, experimentally determined).

Ethylene oxide adds to the catalyst due to reactions IV−VI. At the same time polyethoxylated chains are eliminated from the catalyst together with active sites due to the mechanism the same as that in reaction II. Thus, the total kinetic equation of ethylene oxide units accumulation in the catalyst is as follows:

$$\frac{dN_{EO}}{dt} = k_{ox}N_{A,0}[C_2H_4O]_0(1 + b[OH^-]) + V\left(\frac{dC_A}{dt}\right)\left(\frac{N_{EO}}{N_A}\right) \quad (14)$$

where k_{ox} = rate constant of ethylene oxide addition, L/(mol h); $b = 14$ = rate constants ratio of noncatalyzed to base-catalyzed ethylene oxide addition;[32] $N_{A,0}$ and N_A = the current number of active sites in the catalyst, respectively, mol; N_{EO}/N_A = average number of ethylene oxide units being added per active site of the catalyst.

The rate of catalyst volume changing was obtained by differentiation of the eq 13 taking in account eqs 12 and 14:

$$\frac{dV_i}{dt} = \left(\frac{M_{EO}}{\rho}\right)(k_{ox}N_{A,0}[C_2H_4O]_0(1 + b[OH^-]) - k_d[OH^-]N_{EO}) \quad (15)$$

As it follows from experimental data (Figure 2, A) the activity of the catalyst increases to maximum value during short time after the beginning of the experiment and then slowly decreases during run time. To elucidate the cause of this phenomenon the special experiments were carried out. These experiments were stopped at the moment of maximum catalytic activity, and the values of C_A and M where determined. The results showed that the increase of catalyst activity proceeds due to the increase of carbonate anion fraction in Ionite phase (M) to the maximum value (further marked as M_0). Moreover, it was determined that the values of M_0 lie inside the short range (0.42−0.48) and are independent of process conditions. It was determined (Table 4) that the carbonate anion fraction in the Ionite phase decreases from maximum value (M_0) during the experiments. Presuming the exponential law of changing of M:

$$M = M_0 \exp(-k_M t) \quad (16)$$

the values of the rate constant of the carbonate anion fraction decreasing (further marked as k_M) were calculated and the Arrhenius equation for k_M was obtained:

$$k_M = \exp\left(15.98 - \frac{8804}{T}\right) h^{-1} \quad (17)$$

As a result, the model of deactivation and swelling of the catalyst (Deactivation Model) during the ethylene oxide hydration process was built. The model includes kinetic equations of the elimination of the active sites (eq 12), the change in catalyst volume (eq 15), the change of the number of ethylene oxide units added to the catalyst (eq 14), complemented with equations for the calculation of the current value of carbonate anion fraction in the Ionite phase (eq 16), the current hydroxyl anion concentration in the Ionite phase (eq 10), and the current number of active sites in the catalyst:

$$N_A = C_A V_i \quad (18)$$

Values of k_d and k_{ox} were calculated from the experimental data of final values of C_A and V_i using the Deactivation Model by means of least-squares method. As it follows from Table 4, k_d and k_{ox} depend on temperature and medium composition. The satisfactory description of such dependences was obtained by the following equations:

$$k_d = \frac{a[C_2H_4O]_0}{([H_2O]_0 + [EG]_0)} \exp\left(22 - \frac{6330}{T}\right) \quad (19)$$

$$k_{ox} = [C_2H_4O]_0(b[EO]_0 + c[EG]_0) \exp\left(7.9 - \frac{6023}{T}\right) \quad (20)$$

where: $a = 0.022$; $b = 4.28$; $c = 13.51$.

Moreover the Deactivation Model with determined values of k_d and k_{ox} gives a good description of the current values of C_A during the experiments (lines in Figure 3).

The Deactivation Model complemented with eqs 19 and 20 allows adequate description of experimental data of finite values of C_A and V_i (Table 4).

Reactor Modelling. A combined model of the catalytic reactor consisting of Hydration Model and Deactivation Model above described, was used for design and optimization of industrial tubular reactor of glycol production. Figure 4 illustrates one of the possible schemes of industrial installation, which produces 11.7 tons/h glycol on-stream (38.4% glycol in outlet feed). This five-step reactor scheme can work up to 4000 h with 96−98.3% selectivity and catalyst swelling from 76.2 to 90.1 m^3. Reactors work in adiabatic regime with separated ethylene oxide feed in each reactor. Removal of a heat of reaction proceeds in the intermediate heat exchangers. This technology allows saving about 1.4 tons of high-pressure steam per 1 ton of glycol at the water evaporation stage.

Conclusions

The model of tubular plug-flow fixed-bed catalytic reactor of ethylene oxide hydration with HCO_3^-/CO_3^{2-} -form of anion-exchange resins as the catalyst, including kinetics of the deactivation and swelling of the catalyst has been developed.

This model can be used for design and optimization of different schemes of industrial catalytic reactors of ethylene glycol production.

Received for review May 12, 2005.

OP058005+